Results in Engineering 21 (2024) 101936

Contents lists available at ScienceDirect

Results in Engineering

journal homepage: www.sciencedirect.com/journal/results-in-engineering

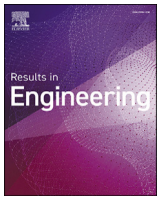

Full Length Article

Numerical analysis of injuries of e-scooter riders in frontal impacts against SUVs

Juan M. Asensio-Gil [a,*], Jesus R. Jimenez-Octavio [a], Alberto Carnicero [a], Manuel Valdano [a], Diego Guzman [b], Francisco J. Lopez-Valdes [a]

[a] MOBIOS Lab, Institute for Research in Technology, Comillas Pontifical University, C. de Santa Cruz de Marcenado, 26, 28015, Madrid, Spain
[b] ICAI School of Engineering, Comillas Pontifical University, C. de Alberto Aguilera, 25, 28015, Madrid, Spain

ARTICLE INFO

Keywords:
E-scooter
Safety
Injury risk criteria
Human body model
SUV
Finite element analysis

ABSTRACT

The rising popularity of e-scooters in urban areas highlights the importance of understanding potential collision dynamics and consequences to enhance rider safety, especially since 80% of fatalities for these vulnerable road users result from incidents involving motor vehicles. This study aims to identify potential injury mechanisms of e-scooter riders involved in frontal impacts against Sports Utility Vehicles (SUVs) using Finite Element Analysis (FEA) and a Human Body Model (HBM). Six impact scenarios at 25 km/h were simulated: on the passenger's side door (1-SD), on the trunk door (2-TD), on the bonnet (3-FB), on the bonnet from the side (4-SB), on the windshield from the side (5-SW), and finally, on the bonnet with an offset (6-FO). A wide range of Injury Risk Criteria (IRCs) was analyzed, including A3MS, HIC15, BrIC, DAMAGE, Cmax and PC Score, and head contact forces were output. Injury Risk Curves were then used to calculate the probability and severity of the sustained injuries predicted by the mentioned IRCs. Overall, the results corresponding to the most injurious scenarios suggested serious (30% to 40% overall probability) and critical (45% probability for the 4-SB scenario) brain, moderate head (30% probability for scenarios 1-SD and 2-TD), and serious thoracic (26% to 78% overall probability) injuries. Additionally, in two scenarios (1-SD and 2-TD), the e-scooter rider's mandible impacted against the vehicle's roof side rail and rear spoiler, involving potential anterior-posterior serious mandible fractures. The conclusions reached in this study help to understand potential injury sources and provide valuable information for the design of specific safety systems or the creation or improvement of e-scooter legislation.

1. Introduction

Over the last years, the popularity of micromobility has experienced rapid growth in urban environments in response to traffic congestion, air pollution and the need for a more affordable and convenient alternative to conventional mobility for short distances. In 2019, 136 million trips were reported in the USA for shared micromobility services, a 60% increase from 2018 [1]. Among these shared services, e-scooters were the most used in 2019 in the USA, with 63.2% of the total, according to the same source.

However, with the rise of these modes of transportation, injuries and road traffic collisions in which they are involved have also become more frequent. Regarding e-scooters, injuries in the USA increased by 507% from 2014 to 2019, reaching 14,919 to 44,338 injured users (95% confidence interval) [2]. These e-scooter-related incidents can involve falls, collisions against static objects, or being impacted by a moving object. Even though crashes involving motor vehicles only account for 8.8% of all injured e-scooter riders [3], they are responsible for 80% of all deaths [4]. Even the integration of e-scooters in the future of urban mobility seems to be challenging, as their detection by autonomous vehicles and advanced driver-assistance systems needs to be significantly improved [5].

In response to these numbers, governments have implemented different regulations regarding the use of e-scooters. Concerning the USA, there are considerable differences among states' current and proposed regulations and definitions for e-scooters [6]. In Europe, Germany legalized e-scooters in 2019, and a maximum speed of 20 km/h and power of 500 W was defined for these vehicles. Additionally, their circulation on the road was allowed, although helmets were not made compulsory [7]. Furthermore, in Spain, the latest update adds to the maximum speed of

* Corresponding author.
E-mail address: jasensio@comillas.edu (J.M. Asensio-Gil).

https://doi.org/10.1016/j.rineng.2024.101936
Received 27 October 2023; Received in revised form 12 February 2024; Accepted 19 February 2024
Available online 23 February 2024

Table 1
Literature review on real-world data of injuries of e-scooter riders.

	Study	[3]	[7]	[13]	[14]	[12]	[10]
Injuries (absolute % per study)	Injured Users	228	76	90	59	180	190
	Head (minor)	38.2	6.6	36.7	33.9	-	-
	Head (concussion)	0.4	3.9	-	6.8	11.7	-
	Head (ICH)	2.2	6.6	6.7	1.7	4.4	-
	Face	5.3	21.1	44.4	20.3	10.6	40
	Face (surgery)	-	5.3	5.6	8.5	2.8	-
	Cervical Spine	0.4	-	-	3.4	0.6	-
	Thorax	1.3	9.2	4.4	6.8	3.3	18
	Upper extremities	19.8	47.4	64.4	50.8	16.7	70
	Lower extremities	5.3	36.8		47.5	17.8	55
	Fractures	31.1	48.6	64.4	31.7	41.7	84
	Mandible (fracture)	-	-	-	3.4	2.2	-
	Tooth (fracture)	-	5.3	-	17.0	6.1	-

25 km/h, the mandatory use of a helmet for all ages under terms yet to be defined, the prohibition of traveling on sidewalks or pedestrian zones, and the inclusion of a circulation certification by 2027 [8]. On the other hand, the French city of Paris banned in April 2023 all shared e-scooter services after a vastly-supported referendum [9].

On user behavior, real data shows a 0.5 to 4.4% rate of helmet use by e-scooter riders during collisions, according to studies conducted in the USA [3,10], Denmark [11], and New Zealand [12] with different duration periods between 2016 and 2019. Combining these studies, 718 e-scooter riders were injured, but only 18 (2.5%) wore a helmet at the moment of the crash. At the time of these studies, helmet use was not compulsory by law in their respective city, state, or country.

Delving into the specific injuries sustained by e-scooter riders, Table 1 summarizes the six most relevant and detailed studies on real-world incidents found in literature, including sample size and occurrence of different types of injury. All proportions refer to the sample size of each study. Head, face, and extremities were the areas with a higher incidence of injuries. As for the severity, head injuries were mainly minor (AIS 1 from the Abbreviated Injury Scale), such as lacerations and contusions, although there were also cases of moderate or serious injuries (AIS 2 and AIS 3), like concussions and intracranial hemorrhages. Additionally, mandible and tooth fractures were observed, with a 2.2 to 3.4% and 5.3 to 17.0% proportion, respectively. Face surgery (excluding dentist-related) was needed in 2.8 to 8.5% of all injured e-scooter riders. Overall, a bone fracture was observed in 31.1 to 84% of the studied e-scooter crashes.

However, understanding the injury mechanisms behind these collisions is key in the mitigation and prevention of them. As highlighted in Nasim et al. [15], both rotational and linear accelerations are involved in head and brain injuries, but only the latter was considered until recently in the current ECE R22.05 motorcycle helmet regulation. Once this new injury mechanism was identified, studies as [15] were able to focus on solutions to mitigate the effect of this mechanism. Another example could be neck hyperextension, one of the main injury mechanisms behind Whiplash Associated Disorders (WADs), and the implementation of cervical airbags in bicycle helmets such as that of study [16]. Hence, an in-depth biomechanical study of e-scooter collisions could provide valuable information for the development of e-scooter safety systems.

Only three previous numerical-simulation-related studies have been found addressing various scenarios involving injuries in e-scooter riders. Matt et al. [17] analyses e-scooter impacts against a curb at different angles using the THUMS Human Body Model (HBM) in LS-Dyna. Similarly, Pasinee et al. [18] studies e-scooters to curb impact kinematics for different dummy model sizes in Madymo. Additionally, Ptak et al. [19] investigates the kinematics involved in e-scooters to Sport Utility Vehicles (SUVs) impacts for two scenarios using Madymo Hybrid-III dummy and e-scooter models and a simplified LS-Dyna vehicle in coupled simulations.

This study aims to identify potential injury mechanisms in e-scooter riders involved in frontal impacts with Sport Utility Vehicles (SUVs) using Finite Element Analysis (FEA) and a Human Body Model (HBM), through a comprehensive set of Injury Risk Criteria (IRCs). To the knowledge of this study, this is the first time a Human Body Model, and not a dummy model, is used for injury characterization in e-scooter impacts against a motor vehicle. This allows for a more in-depth and precise analysis of the sustained injuries in potentially fatal e-scooter collision scenarios, a noble approach that provides valuable information as the main original contribution of this study for the improvement of current legislation or the creation of specific active or passive safety systems, among others.

2. Material and methods

2.1. Software and hardware

For all numerical simulations, the FEA method was used. In particular, the explicit-based software package LS-Dyna MPP v9.3.1 with single precision was selected. On the hardware side, 88 HPC (High Performing Computing) cluster cores were assigned to this study.

2.2. Collision scenarios and boundary conditions

Six scenarios regarding e-scooter frontal impacts against an SUV were defined and simulated. These were: (1-SD) impact on the passenger's side door at the point of maximum height of the vehicle, (2-TD) impact on the trunk door, (3-FB) impact on the bonnet from the front, (4-SB) impact on the bonnet from the side aligning the head of the e-scooter's rider with the motor block, (5-SW) impact on the lower part of the windshield from the side, and (6-FO) impact on the bonnet from the front with an offset so that the e-scooter rider impacts with more rigid elements of the vehicle. These scenarios are superpositioned in Fig. 1.

In all cases, the e-scooter initial velocity was set to 25 km/h, considering the regulations in European countries regarding e-scooters. On the other hand, the motor vehicle was stationary. Additionally, no helmet was included for the e-scooter rider, considering the most restrictive case found in the heterogeneous governments' regulations and their aforementioned generalized lack of use by the e-scooter rider community. Furthermore, gravity was considered for all components of the simulation. For all scenarios, the total simulation time was set to 500 ms to address the rider-vehicle impact adequately.

2.3. Modeling components

2.3.1. E-scooter model

An e-scooter finite element model was developed by measuring the Segway Ninebot Kickscooter eS2, a worldwide available commercial e-scooter. The physical e-scooter was disassembled in three parts to accurately capture its mass distribution, inertia tensor, and the position of

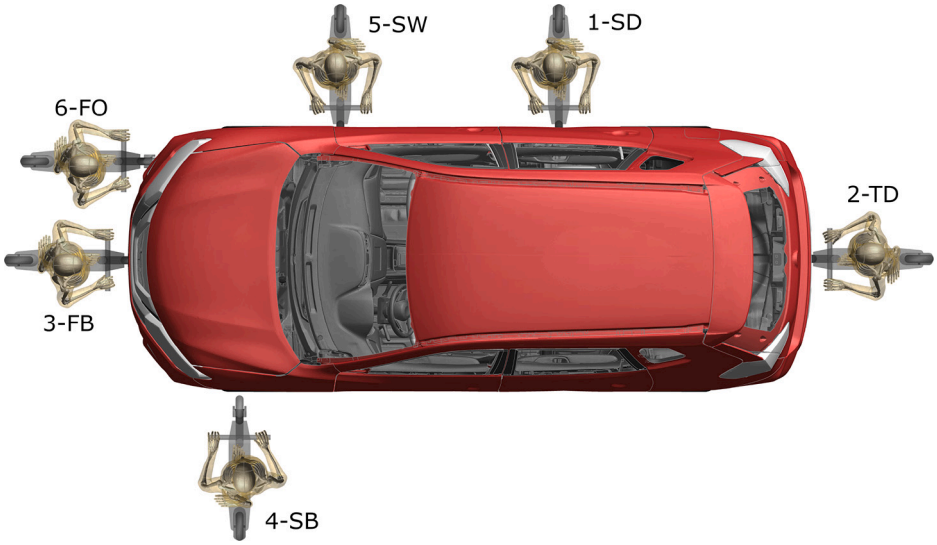

Fig. 1. Analysed impact scenarios.

Table 2
E-scooter specifications.

	Mass [kg]	Center of mass [mm]	Inertia tensor [kg mm^2 × 10^3]
Part 1	3.15	(620.0, 0.0, 0.0)	$\begin{bmatrix} 20.2 & 0.0 & -27.0 \\ 0.0 & 411.6 & 0.0 \\ -27.0 & 0.0 & 409.0 \end{bmatrix}$
Part 2	3.22	(0.0, 0.0, 0.0)	$\begin{bmatrix} 4.3 & 0.0 & 0.0 \\ 0.0 & 7.8 & 0.0 \\ 0.0 & 0.0 & 4.3 \end{bmatrix}$
Part 3	5.18	(100.0, 0.0, 498.9)	$\begin{bmatrix} 463.0 & 0.0 & -10.6 \\ 0.0 & 456.4 & 0.0 \\ -10.6 & 0.0 & 9.4 \end{bmatrix}$
Total	11.55	(213.9, 0.0, 223.8)	$\begin{bmatrix} 1407.8 & 0.0 & -345.4 \\ 0.0 & 2338.3 & 0.0 \\ -345.4 & 0.0 & 964.9 \end{bmatrix}$

Fig. 2. Exploded view of e-scooter model: Parts 2, 1 and 3 (left to right).

the center of gravity (CoG). These parts included the stem, battery and handlebar (Part 1), the front motor wheel (Part 2), and the deck and rear wheel (Part 3), as observed in Fig. 2. The e-scooter virtual model (Fig. 3) consists of 32,574 shell elements with non-deformable standard aluminum as their assigned material.

Additionally, a revolute joint was defined for the motor wheel, and the handlebar height was adjusted to fit the selected e-scooter rider virtual model ergonomically. Consequently, the e-scooter model's main specifications included an 11.55 kg total mass, a 120.49 cm handlebar height, an 80.08 cm wheel-to-wheel distance, and a 20.32 cm wheel diameter. Additionally, Table 2 summarizes the main physical properties of the model, where the origin of the coordinate axes used in the study is located in the frontal motor wheel's geometrical center. The X-axis follows the longitudinal direction of the e-scooter, whereas the Z-axis follows the vertical direction.

2.3.2. Motor vehicle model

The vehicle model selected was the 2020 Nissan Rogue version 1, a detailed open-source model developed in 2021 by the Center for Collision Safety and Analysis (CCSA) of George Mason University (GMU) in collaboration with the National Highway Traffic Safety Administration (NHTSA), as shown in Fig. 4. This model consists of 3,088,092 elements. Among these, the elements that interact with the other modeling components are shell-type. Its representability as a Sport Utility Vehicle (SUV) was analyzed by comparing its silhouette to that of the general SUV vehicle of the Euro NCAP's TB024 certification protocol. This comparison was only performed from the beginning at the front until the end of the windshield, considering the parametrization scope of the mentioned reference SUV vehicle. From that reference, an offset of 75 mm for each side was computed to serve as a corridor for the selected vehicle model's silhouette. Fig. 5 shows how the Nissan Rogue overall falls inside these offsets.

2.3.3. E-scooter rider model

The most recent version of the Toyota THUMS pedestrian 50th percentile male HBM was chosen for this study, corresponding to v4.0.2 of January 2021 and with 1,976,359 elements. The variant without fractures was considered. A pre-simulation was performed to position the model as an e-scooter rider. Among the various foot placement config-

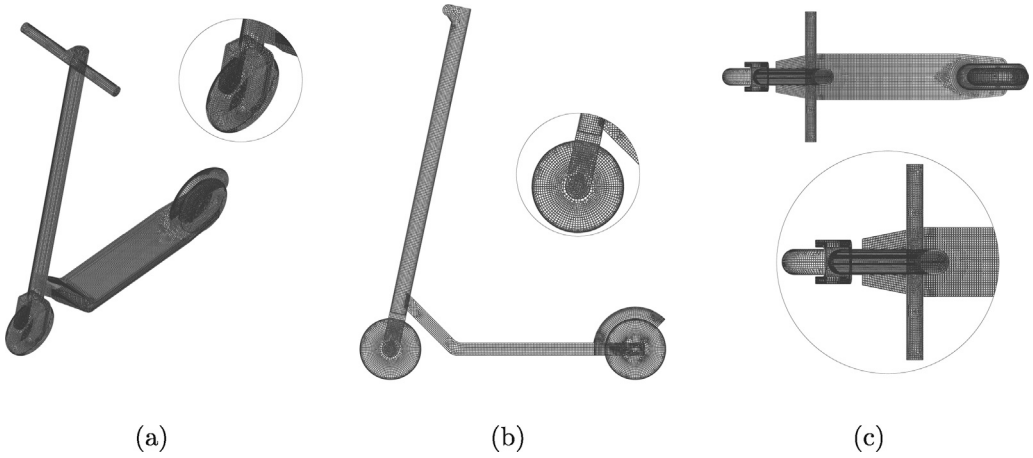

Fig. 3. E-scooter model ISO view (a), Lateral view (b) and Top view (c).

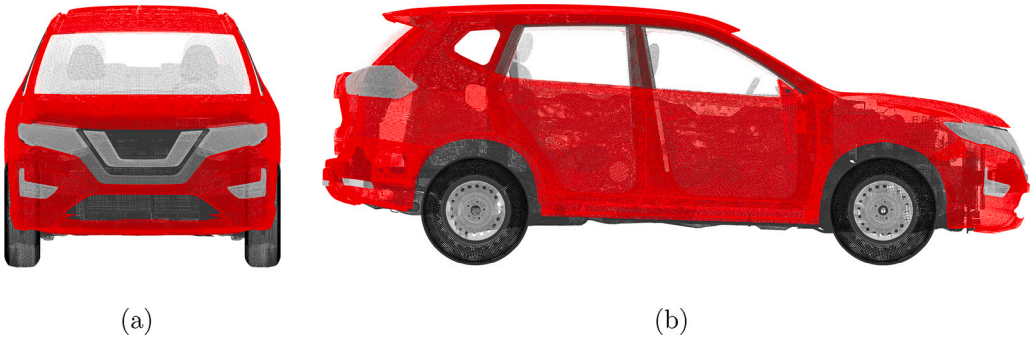

Fig. 4. Motor vehicle model (a) Front view (b) Lateral view.

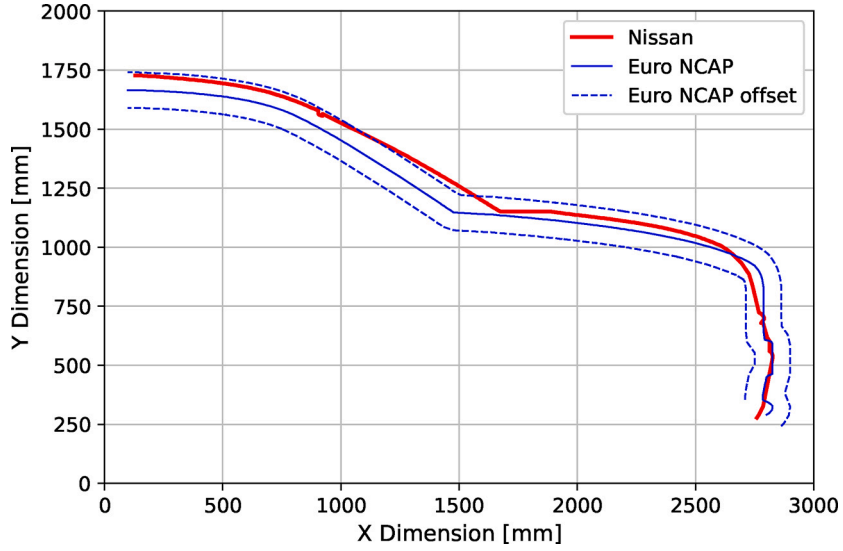

Fig. 5. Motor vehicle model silhouette comparison against reference.

urations found in the real world, the tandem style with the front toes forward and the rear toes angled was selected, following the 75% occurrence observed in the study by Ittai et al. [20]. Additionally, a hand grip was added to the model.

2.4. Injury risk criteria

The injury assessment focused on the head, face and thorax regions, following the most recurrent and severe injuries observed in the real-world e-scooter-related incident data gathered in section 1. Thus, the IRCs analyzed included the 3-millisecond acceleration of the head CoG (A3MS), the Head Injury Criterion (HIC15), the Brain Injury Criterion (BrIC), the Diffuse Axonal Multi-Axis General Evaluation (DAMAGE), the Cmax and the Principal Component (PC) Score. These IRCs were later translated to injury severity using the AIS scale [21]. Additionally, head contact forces were studied to predict the likelihood of mandible fractures.

2.5. Simulation setup and parameters

The simulation setup in LS-Dyna was based on an explicit dynamic analysis with the central difference method time integration scheme. The internal energy dissipated by viscosity was included in the energy balance. Hourglass energy, rigid wall energy, sliding interface energy dissipation, Rayleigh energy, and initial reference geometry energy were also considered in the energy balance. The time step of the simulation was adaptative with a scale factor of 0.9 to improve numerical stability and a minimum time step of 4.44E-4 was defined. This minimum time step selected was that of the HBM, considered the most complex model in the system (the minimum time step of the vehicle model was greater).

The contacts to define the interaction between the different components of the simulated system were based on common practices in biomechanics and impact simulation research derived from the existing literature, including the LS-Dyna and THUMS HBM manuals. The contact between the vehicle and the floor was not modified from the original model. Overall, friction was set to 0.3 and viscous damping to 20.0, following the Technical Bulletin 024 of EuroNCAP [22] and Östh et al. [23], respectively. The contact between the e-scooter and the floor was defined as a rigid body one way to rigid body, as both of these components were rigid bodies. The remaining contacts were defined as automatic surface to surface, following the official recommendations of LS-Dyna for crash analysis and THUMS HBM ([24] and [25]). For contacts involving the HBM, the penalty stiffness was not modified from the default value [25]. However, the value of the penalty stiffness was three times increased for the e-scooter to vehicle contact to better capture the overall stiffness behavior of the parts that form these two more rigid components.

3. Theoretical foundation

This section describes theoretical considerations regarding the proposed injury assessment of this study.

3.1. Abbreviated injury scale (AIS)

The Abbreviated Injury Scale (AIS) is a widely used tool in the field of trauma medicine and injury and biomechanics research to categorize and quantify the severity of injuries. It provides a standardized and systematic way to assess injuries based on their anatomical and physiological characteristics. The AIS classifies injuries on a scale from 1 to 6, with each level representing a different degree of severity: Minor (AIS 1), Moderate (AIS 2), Serious (AIS 3), Severe (AIS 4), Critical (AIS 5), and Maximum (AIS 6). These levels signify varying degrees of anatomical disruption and physiological impact. The severity levels are specific to the body region assessed, making direct comparisons between, for instance, an AIS 2 head injury and an AIS 2 chest injury impossible. This ensures a more accurate assessment of the overall impact of injuries on an individual. Additionally, an AIS 9 designation is used when the severity of an injury is unknown or cannot be determined, and an AIS 0 is associated with no injury sustained.

3.2. Head injuries

In this study, the A3MS (3-millisecond acceleration of the head CoG) criterion was addressed following the Post Mortem Human Subject (PMHS) tests of Got et al. [26] that suggest a value of 80g as the minor head injury threshold (AIS 1) and 130g as a threshold value for a serious (AIS 3) injury. Based on the results in the study [26], the current study assumed that A3MS values above these two thresholds resulted in a 100% probability of AIS 1 and AIS 3, respectively. Moreover, the HIC (Head Injury Criterion) was calculated using equation 1 [27], and the associated probability and severity of head injuries was addressed using Hayes et al. [28], where the associated injury risk curves were gathered from PMHS studies and validated by real-world data on vehicle-to-pedestrian collisions.

$$HIC_{15} = \max_{(t_1,t_2)} \left\{ \left[\frac{1}{t_2 - t_1} \int_{t_1}^{t_2} a(t)dt \right]^{2.5} (t_2 - t_1) \right\} \quad (1)$$

3.3. Brain injuries

Regarding the BrIC (Brain Injury Criterion), its value was calculated using equation 2 [29]. In this equation, ω_x, ω_y and ω_z are the maximum angular velocities of the c.o.g. of the head in each axis, and $\omega_{x\,cr}$, $\omega_{y\,cr}$ and $\omega_{z\,cr}$ refer to the critical values for each direction. The maximum principal strain (MPS) based critical values 66.30, 53.80 and 41.50 rad/s were considered, following the conclusions drawn in Takhounts et al. [29]. This same study was followed to address brain injury probability and severity via injury risk curves in the different impact scenarios. Additionally, The DAMAGE (Diffuse Axonal Multi-Axis General Evaluation) brain injury criterion values were calculated following Gabler et al. [30]. This criterion considers the maximum brain strain due to angular motion in each axis as a second-order physical mass-spring-damper system. Then, the equations of motion under forced excitation are solved (equation 3), where $\delta(t)$ is the displacement vector solution of the mentioned equations, and β is a scale factor used to fit the metric to maximum brain strain (MPS). This metric was translated into injury probability and severity using the injury risk curves for AIS 2 and AIS 4+ levels of the Technical Bulletin 35 of Euro NCAP [31].

$$BrIC = \sqrt{\left(\frac{\omega_x}{\omega_{x\,cr}}\right)^2 + \left(\frac{\omega_y}{\omega_{y\,cr}}\right)^2 + \left(\frac{\omega_z}{\omega_{z\,cr}}\right)^2} \quad (2)$$

$$DAMAGE = \beta max_t \left\{ \left| \vec{\delta}(t) \right| \right\} \quad (3)$$

3.4. Thoracic injuries

The Cmax and PC Score (Principal Components Score) thoracic injury criteria were assessed in this study following Poplin et al. [32] and Piqueras et al. [33]. The study [32] compared a PMHS test dataset with both criteria applied to the IR-TRACC sensors of a THOR 50th percentile ATD (Anthropometric Test Device) and formulated an AIS 3+ injury probability index included for both metrics, with the expression included in Table 3. In this equation, x is the value obtained for the metric (Cmax or PC Score), and β and λ are the parameters associated with the survival model of each metric. The age considered for the e-scooter rider was 50 years old. These criteria and their associated injury estimated probability was implemented in the current study following the study [33], by including in the HBM output nodes on the

Table 3
Summary of the Theoretical Foundation.

Metric	Area	Comments	Injury assessment	References
A3MS	Head	Threshold definition based	80g (AIS 1 100%), 130g (AIS 3 100%)	[26]
HIC15	Head	Vehicle to pedestrian based	Injury Risk Curves	[27,28]
BrIC	Head	MPS based	Injury Risk Curves	[29]
DAMAGE	Head	Euro NCAP TB035	Injury Risk Curves (AIS 2 & AIS 4+)	[30,31]
Cmax	Thorax	Adapted to HBM	$P(AIS3+\mid x)=1-e^{-\left[\frac{x}{e^{4.778-0.017*50}}\right]^{3.356}}$	[32,33]
PC Score	Thorax	Adapted to HBM	$P(AIS3+\mid x)=1-e^{-\left[\frac{x}{e^{2.868-0.018*50}}\right]^{3.311}}$	[32,33]
Contact Force	Mandible	Variable comparison based	PMHS test datasets from references	[34,36]

4th and 8th ribs bilaterally. The Cmax metric was obtained as the absolute maximum peak resultant deflection out of the four HBM output nodes, whereas the PC Score was obtained following equation 4 [32]. In this equation, UP_{tot} and LOW_{tot} are the time-independent sums of peak values for the upper and lower deflections, respectively, UP_{dif} and LOW_{dif} are the absolute time-dependent maximums of the difference between the left and right sides, l_n are the principal component loadings, and s_n are the standard deviations of the deflection metrics.

$$PC\,Score = l_1\left(\frac{UP_{tot}}{s_1}\right)+l_2\left(\frac{LOW_{tot}}{s_2}\right)+l_3\left(\frac{UP_{dif}}{s_3}\right)+l_4\left(\frac{LOW_{dif}}{s_4}\right) \quad (4)$$

3.5. Mandible injuries

Head contact force was also included in this study to address the potential for mandible fractures, an injury fairly present in the aforementioned gathered real-world data on e-scooter incidents. Three experimental studies [34–36] were identified in the literature that used PMHS data to address and analyze mandible fractures. These studies characterized mandible fractures based on various parameters, such as impact force and energy, impact velocity and direction relative to the mandible, and contact area. However, for the present study, only Nahum [34] and McElhaney et al. [36] were considered, as the study [35] analyzed high-velocity impacts ranging from 33 to 50 m/s, which were not relevant to the current analysis. The present study assumed that in the simulated scenarios where the mandible-related impact parameters could be considered comparable with those of a PMHS test from the mentioned references, the severity of the fracture (if present) from that PMHS test would be expected in the correspondent simulation scenario, and its associated probability would be of 100%.

In addition, Table 3 shows a summary of the described Theoretical Foundation.

4. Results

Table 4 shows the afore-described IRCs for each scenario and Table 5 summarizes their correspondent AIS severity and probability (if available). Only injuries with a probability higher than 5% were considered. Subsequently, potential head, thorax and mandible injuries associated with the simulated scenarios are analyzed.

4.1. Head injuries

Regarding A3MS and HIC, the most injurious scenario was the impact on the passenger's side door (1-SD), reaching an AIS 1 and having a 30% probability of AIS 2 injuries, as suggested by A3MS and HIC15 criteria, respectively. The subsequent two scenarios with higher head injury metrics were the impact on the trunk door (2-TD) and the impact on the bonnet (3-FB), where only the HIC15 criterion predicted an injury, in the first case an AIS 2 injury with a 30% probability, and in the second case an AIS 1 injury with a 35% probability. Both IRC metrics found no significant injury in the rest of the scenarios.

Table 4
Values obtained for the IRCs from the simulations.

IRC	Units	1-SD	2-TD	3-FB	4-SB	5-SW	6-FO
A3MS	[g]	79.04	58.37	71.79	40.51	26.65	20.61
HIC15	[-]	409.58	434.6	261.57	82.91	24.19	18.18
BrIC	[-]	0.70	0.76	0.73	1.06	0.72	0.69
DAMAGE	[-]	0.41	0.36	0.37	0.37	0.18	0.19
Cmax	[mm]	57.26	46.27	37.95	40.50	53.25	44.62
PC Score	[-]	7.16	5.63	4.99	5.37	6.57	5.69

4.2. Brain injuries

Moreover, BrIC and DAMAGE criteria showed some discrepancies in injury severity and probability. On the one hand, the DAMAGE metric suggested AIS 2 injuries with a significant probability in the first four scenarios (1-SD, 2-TD, 3-FB and 4-SB). In this case, the most injurious scenario was the first one with a 45% probability, 5% more than the rest of the mentioned scenarios. On the other hand, the BrIC metric suggested a 30% to 40% probability of AIS 3 injuries across all scenarios, except for the impact on the bonnet from the side (4-SB). In this case, a 45% probability of AIS 5 injury was estimated.

4.3. Thoracic injuries

The results show consistency among Cmax and PC Score metrics, although Cmax predicts a higher probability of AIS 3 thoracic injury for all scenarios. The most injurious scenarios were 1-SD and 5-SW, showing for an AIS 3 injury, a 63 and a 53% probability for PC Score and a 78 and a 69% probability for Cmax, respectively. The rest of the scenarios range in AIS 3 probability from 26 to 37% for PC Score and from 31 to 52% for Cmax.

4.4. Mandible injuries

The association of mandible-vehicle peak contact force with mandible fracture needs the analysis of the impact force and energy, the impact velocity and direction with respect to the mandible, and the contact area. Thus, a combination of quantitative and qualitative output data is required. To this end, Figs. 6 to 8 are shown. These illustrations correspond to frames of interest for each scenario, such as the peak mandible-vehicle contact force frame.

The head-vehicle contact force signal in the impact on the passenger's side door (1-SD) and the impact on the trunk door (2-TD) scenarios showed three and two different peaks, respectively. In both cases, the

Table 5
Severity [AIS] and Probability [%] of injury for each scenario and IRC.

	1-SD	2-TD	3-FB	4-SB	5-SW	6-FO
A3MS	1 (100%)	0	0	0	0	0
HIC15	2 (30%)	2 (30%)	1 (35%)	0	0	0
BrIC	3 (30%)	3 (40%)	3 (35%)	5 (45%)	3 (35%)	3 (30%)
DAMAGE	2 (45%)	2 (40%)	2 (40%)	2 (40%)	<2	<2
Cmax	3 (78%)	3 (52%)	3 (31%)	3 (37%)	3 (69%)	3 (48%)
PC Score	3 (63%)	3 (36%)	3 (26%)	3 (32%)	3 (53%)	3 (37%)

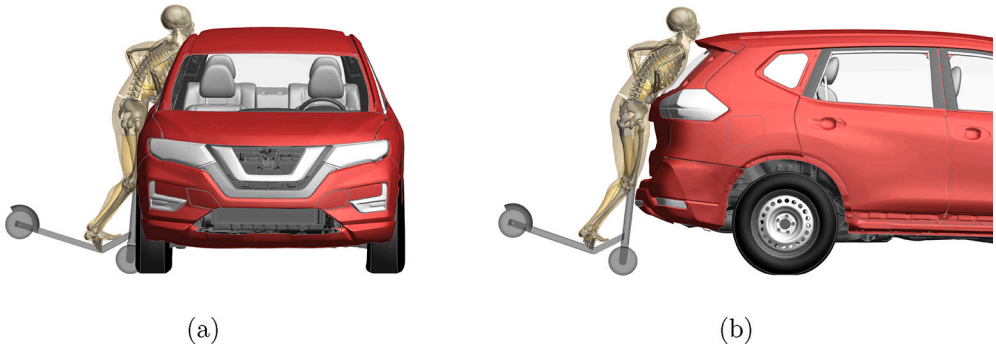

Fig. 6. Scenarios 1-SD (a) and 2-TD (b).

Fig. 7. Scenarios 3-FB (a) and 4-SB (b).

Fig. 8. Scenarios 5-SW (a) and 6-FO (b).

first and highest of them corresponded to an anterior-posterior impact on the mandible (Figs. 6-a and 6-b). For these mandible impacts, the recorded impact forces were 5.16 and 5.26 kN, the impact energies were 85.70 and 40.26 J, the impact velocities were 7.72 and 7.68 m/s and the contact areas were 22.38 and 21.40 cm^2, respectively.

In the case of the impact on the bonnet from the front 3-FB, the first and highest impact (out of two) was produced in the anterior-posterior direction on the mandible area (Fig. 7-a), as in the previous two scenarios. In this case, the impact force was 1.45 kN, the impact energy was 50.3 J, the impact velocity was 7.34 m/s, and the contact area was 25.83 cm^2.

Furthermore, in the impact on the bonnet from the side 4-SB (Fig. 7-b), the head contact between the rider and the motor vehicle was only located in the parietal skull bone region and not in the mandibular one. Consequently, mandible-vehicle contact forces were not assessed.

In the impact on the windshield from the side scenario 5-SW (Fig. 8a), the e-scooter rider-vehicle impact head regions were the frontal skull and maxilla bones. Similarly, the head contact region on the impact bonnet with an offset scenario 6-FO (Fig. 8-b) was observed to be located in the frontal bone area.

Table 6 summarizes the main characteristics of the observed impact peaks for each scenario. In the impact region field, MB stands for mandible bone, MX for maxilla bone, P for parietal bone, and F for frontal bone, whereas in the direction field, AP stands for anterior-posterior and O for oblique.

Table 6
Summary of the observed head-vehicle contacts.

	1-SD		2-TD		3-FB		4-SB	5-SW		6-FO
Peak No.	1	2 & 3	1	2	1	2	1	1	2	1
Region	MB	MX	MB	MX	MB	F	P	F	MX	F
Direction	AP	AP	AP	AP	AP	AP	O	AP	AP	O

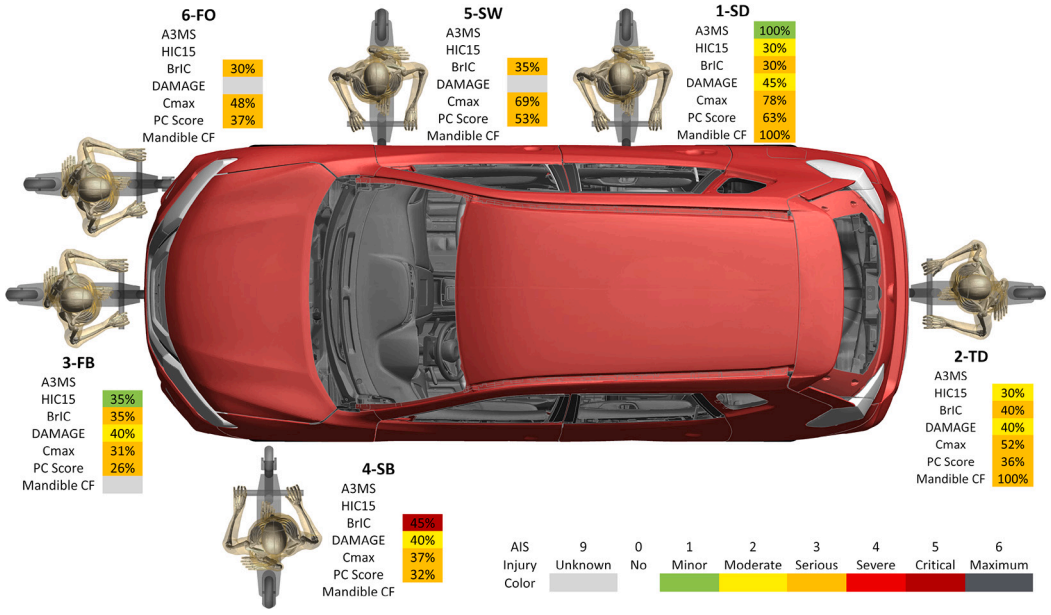

Fig. 9. Summary of results.

Table 7
Summary of mandible bone fracture assessment.

	Units	1-SD	2-TD	3-FB
Force	[kN]	5.16	5.26	1.45
Energy	[J]	85.70	40.26	50.30
Velocity	[m/s]	7.72	7.68	7.34
Area	[cm^2]	22.38	21.40	25.83
Fracture	[-]	Yes	Yes	Unknown
AIS	[-]	3	3	-

On mandible fracture assessment, the results obtained for the first two scenarios (1-SD and 2-TD) had, in comparison with the study [34], greater in terms of impact force, energy and velocity. Thus, an AIS 3 mandible fracture with a probability of 100% was predicted for both cases. Nevertheless, when comparing the results of the third scenario (3-FB) with the mentioned literature studies, no conclusions on mandible fracture could be drawn, as energy and velocity impact values were greater, but the recorded impact force fell below the given range. The contact area in the three simulations was considered as sufficiently similar to that of the study [34]. Table 7 summarizes the results of the mandible fracture assessment.

Finally, Fig. 9 shows a graphical summary of all the results obtained in this study.

5. Discussion

5.1. Head and brain injuries

The results observed for A3MS and HIC criteria were consistent among scenarios in terms of injury risk and other quantitative and qualitative factors. Nonetheless, BrIC and DAMAGE criteria offered some discrepancies among each other in injury severity and in which scenarios should be considered as more injurious. There are two factors to take into account regarding this observation that could explain these dissimilarities in both injury criteria. First, no AIS 3 injury risk curve was found for the DAMAGE criterion, hindering a fair comparison against BrIC injury prediction results. Second, the impact scenarios simulated in the present study showed overall rapid angular velocities but with low angular accelerations, especially in the impact on the bonnet from the side 4-SB scenario. Nevertheless, Gabler et al. [30] analyzed the head injury predictions of an HBM in multiple impact scenarios and concluded that the DAMAGE criterion correlated better in the estimation of brain MPS than the BrIC criterion, with a significant difference in pedestrian impact conditions (closest in boundary conditions to e-scooter impacts in standard impact tests datasets). Thus, the DAMAGE criterion should be considered above the BrIC criterion for characterizing head injury in the present study. Overall, BrIC and DAMAGE criteria predict significantly higher head injury severities than A3MS and HIC, suggesting a prevalence of head rotation-related injuries over those potentially caused by translation in the simulated scenarios.

5.2. Thoracic injuries

The Cmax criterion suggested higher injury probability than PC Score across all scenarios. Nevertheless, PC Score takes into account asymmetric loads and, thus, is a more complete and accurate thoracic injury criterion than Cmax [32], especially when addressing oblique impacts [33]. Hence, the PC Score should be considered above Cmax for characterizing thoracic injury in this particular study. The asymmetric thoracic loads observed in the simulated scenarios were caused by the initial position of the e-scooter rider, which forced the handlebar of the e-scooter to make oblique contact with the abdominal region and, subsequently, rotate the torso of the rider before impact. However, in scenarios 3-FB and 4-SB, one of the user's arms interacted with the vehicle, reducing this rotation of the torso and, consequently, significantly decreasing the oblique component of the impact. As a result, the differ-

ence between both Cmax and PC Score regarding injury probability for AIS 3 severity was reduced from 16% in other scenarios to 5%.

5.3. Mandible injuries

In addition, three of the simulated e-scooter collision scenarios (1-SD, 2-TD and 3-FB) involved a direct impact of the mandible against the motor vehicle. In particular, the involved vehicle areas were the roof side rail, the rear spoiler and the bonnet. For the first two cases, an AIS 3 anterior-posterior mandible fracture was predicted. Recorded impact forces and energies were significantly high, which seems coherent with the high stiffness of the impacted vehicle areas. However, for the mandible impact involving the bonnet, no injury could be determined as it was not possible to match the obtained values with the literature. These results seem to suggest that a standard open-face helmet may have limited effectiveness in preventing facial fractures because of the exposure of the mandible. Several studies regarding motorcycles (Wu et al. [37]) and bicycles (Sorenson et al. [38] and Stier et al. [39]) agree on the lack of prevention or mitigation of facial injuries when using an open-face helmet and the need to make integral helmets mandatory. Future work comparing facial injury mitigation in open-face and integral helmets with PMHS testing may be needed to further investigate this.

5.4. Considerations

Overall, the obtained results initially seem not to match the observed real-world injuries gathered from the literature. However, the type of incidents analyzed in this study has been found to account only for 8.8% of total e-scooter collisions but also for 80% of all e-scooter rider deaths, as previously mentioned. Unfortunately, there is no data on injury occurrence in these fatal incidents.

Nonetheless, there are some limitations to this study. As agreed by the National Transportation Safety Board, there is a general lack of trip, injury and user behavior data related to e-scooters [40]. This limits the ability to define scenarios and boundary conditions accurately and necessitates relying on the best available knowledge. Therefore, the results of this study should be considered as a first step towards understanding the biomechanics of e-scooter riders in impacts against SUVs.

Furthermore, the simulations did not consider muscle activation and response time, as insufficient input on these characteristics related to e-scooter drivers was available. On the one hand, muscle activation could impact the simulations with the evolution in time of the defined initial grip, among other user-behavior-related factors. On the other hand, most of the proposed impact scenarios in this study account for the e-scooter rider being absent-minded or unable to predict the collision. Thus, whether the e-scooter rider could significantly modify any activation-related event is uncertain.

Additionally, the translation of IRCs and other metrics into injury probability and severity in this study was performed considering, when possible, the context of e-scooter collisions. There are usually two key factors that affect the applicability of a specific set of injury risk curves to assess the values obtained for its respective injury criterion. On the one hand, whether that criterion was conceived for an ATD or an HBM or whether the selected set of injury risk curves accounts for this. On the other hand, the context in which the injury risk curves were validated (pedestrian or car occupant, direction of impact or distance from the impact).

For instance, the selected injury risk curves associated with the HIC criterion of Hayes et al. [28] were calibrated for HBMs and validated by real-world data on vehicle-to-pedestrian collisions. Similarly, the boundary conditions from the PMHS tests conducted by Got et al. [26] and Nahum [34] and McElhaney et al. [36], which enabled the current study to define the thresholds for A3MS and to predict mandible fractures, respectively, could be considered comparable to those of the simulated scenarios, especially on those where a more rigid vehicle surface was involved. In addition, the DAMAGE criterion and injury risk curves were created for their application on HBMs and validated using a correlation with MPS on a wide range of different impact conditions, including vehicle-to-pedestrian [30].

Regarding BrIC, the selected injury risk curves proposed in the study [29] accounted for an HBM but showed a lower correlation to MPS than those of the DAMAGE criterion in vehicle-to-pedestrian collisions [30]. Cmax and PC Score AIS 3+ injury risk equations from Poplin et al. [32] were conceived for THOR ATDs, and even though their applicability to HBMs was demonstrated in the study [33], the PMHS test datasets used as a reference in both studies involved occupant protection.

Moreover, this study proposes future work to analyze further and understand injury mechanisms in e-scooter crashes involving motor vehicles. First, dummy and PMHS experimental testing could help provide more information on the interaction between the system components in this type of incident. Second, this study covers a wide range of collisions of e-scooter frontal impacts against an SUV. However, oblique impacts fall out of scope, needing further research to address injury mechanisms related to them.

6. Conclusions

Six different scenarios of e-scooter frontal impacts against an SUV at 25 km/h were simulated. An e-scooter model developed by reverse engineering, the THUMS AM50 v4.0.2 HBM and an FE model of the 2020 Nissan Rogue were utilized as modeling components. The major findings suggested by the results of this study include:

- Serious brain injuries across all scenarios with a probability ranging from 30% to 40%, except for scenario 4-SB where a 45% probability of critical brain injury was obtained.
- Moderate head injuries with a probability of 30% for scenarios 1-SD and 2-TD.
- Serious thoracic injuries sustained in all scenarios, with probabilities ranging from 26% to 78%.
- Potential serious mandible anterior-posterior fractures in scenarios 1-SD and 2-TD.

These findings should help to understand potential injury sources for e-scooter riders as this means of transportation becomes more popular. Moreover, they could provide valuable information for the design of specific safety systems or the creation or modification of e-scooter legislation. Future recommendations include dummy and PMHS experimental testing to help provide more information on the interactions between the components of the system.

CRediT authorship contribution statement

Juan M. Asensio-Gil: Writing – review & editing, Writing – original draft, Visualization, Validation, Supervision, Software, Project administration, Methodology, Investigation, Formal analysis, Data curation, Conceptualization. **Jesus R. Jimenez-Octavio:** Writing – review & editing, Validation, Supervision, Resources, Funding acquisition, Conceptualization. **Alberto Carnicero:** Writing – review & editing, Validation, Supervision, Resources, Funding acquisition, Conceptualization. **Manuel Valdano:** Software, Methodology. **Diego Guzman:** Software. **Francisco J. Lopez-Valdes:** Writing – review & editing, Validation, Supervision, Conceptualization.

Declaration of competing interest

The authors declare that they have no known competing financial interests or personal relationships that could have appeared to influence the work reported in this paper.

Data availability

No data was used for the research described in the article.

Acknowledgements

The authors would like to express their gratitude to Centro de Experimentación y Seguridad Vial de MAPFRE, CESVIMAP (project TIBET) and Comillas Pontifical University (project IASPE) for their partial funding of this research.

References

[1] National Association of City, Transportation Officials (NACTO), Shared Micromobility in the US: 2019 (2019).
[2] K.X. Farley, M. Aizpuru, J.M. Wilson, C.A. Daly, J. Xerogeanes, M.B. Gottschalk, E.R. Wagner, Estimated incidence of electric scooter injuries in the US from 2014 to 2019, JAMA Netw. Open 3 (8) (2020) e2014500, https://doi.org/10.1001/jamanetworkopen.2020.14500.
[3] T.K. Trivedi, C. Liu, A.L.M. Antonio, N. Wheaton, V. Kreger, A. Yap, D. Schriger, J.G. Elmore, Injuries associated with standing electric scooter use, JAMA Netw. Open 2 (1) (2019) e187381, https://doi.org/10.1001/jamanetworkopen.2018.7381.
[4] International Transport Forum (ITF), Safe Micromobility (2020).
[5] S. Gilroy, D. Mullins, E. Jones, A. Parsi, M. Glavin, E-scooter rider detection and classification in dense urban environments, Results Eng. 16 (2022) 100677, https://doi.org/10.1016/j.rineng.2022.100677.
[6] Alabama Transportation Policy Research Center, Scooter laws by state (2019).
[7] P. Störmann, A. Klug, C. Nau, R.D. Verboket, M. Leiblein, D. Müller, U. Schweigkofler, R. Hoffmann, I. Marzi, T. Lustenberger, Characteristics and injury patterns in electric-scooter related accidents: a prospective two-center report from Germany, J. Clin. Med. 9 (5) (2020), https://doi.org/10.3390/jcm9051569.
[8] Boletín Oficial del Estado (BOE), 18, Real Decreto 970/2020, of November 10, of the Dirección General de Tráfico, which approves the Characteristics Manual for personal mobility vehicles, 2022.
[9] Conseil de Paris, Report of the control commission - Vote of April 2, 2023, E-scooters services in Paris, 2023.
[10] Austin Public Health, Dockless Electric Scooter-Related Injuries Study, Epidemiology and Public Health Preparedness Division, 2019.
[11] S.N. Blomberg, O. Rosenkrantz, F. Lippert, H. Christensen, Injury from electric scooters in Copenhagen: a retrospective cohort study, BMJ Open 9 (2019), https://doi.org/10.1136/bmjopen-2019-033988.
[12] A. Brownson, P. Fagan, S. Dickson, I. Civil, Electric scooter injuries at Auckland city hospital, New Zealand Med. J. 132 (2019) 62–72.
[13] B. Trivedi, M. Kesterke, R. Bhattacharjee, W. Weber, K. Mynar, L. Reddy, Craniofacial injuries seen with the introduction of bike-share electric scooters in an urban setting, J. Oral Maxillofac. Surg. 77 (2019), https://doi.org/10.1016/j.joms.2019.07.014.
[14] A. Harbrecht, M. Hackl, T. Leschinger, S. Uschok, K. Wegmann, P. Eysel, L. Mueller, What to expect? Injury patterns of electric-scooter accidents over a period of one year - a prospective monocentric study at a level 1 trauma center, Eur. J. Orthop. Surg. Traumatol. 32 (2022), https://doi.org/10.1007/s00590-021-03014-z.
[15] M. Nasim, M.J. Hasan, U. Galvanetto, Impact behavior of energy absorbing helmet liners with pa12 lattice structures: a computational study, Int. J. Mech. Sci. 233 (2022) 107673, https://doi.org/10.1016/j.ijmecsci.2022.107673.
[16] C.M. Vives-Torres, M. Valdano, J. Alvarez-Fernandez, J.M. Asensio-Gil, C. Rodriguez-Morcillo, M. Millet-Solanelles, N. Oleaga-Ortega, L. Llobet-Cusí, F.J. Lopez-Valdes, The effectiveness of cervical airbags in the control of head and neck kinematics, in: Proceedings 23: International Research Council on Biomechanics of Injury Conference, International Research Council on Biomechanics of Injury (IRCOBI), 2023, p. 55.
[17] P. Matt, M. Jenerowicz, T. Schweiger, F. Heisch, J. Lienhard, M. Boljen, Investigation of e-scooter drivers colliding with kerbs: a parametric numerical study, in: Proceedings 22: International Research Council on Biomechanics of Injury Conference, International Research Council on Biomechanics of Injury (IRCOBI), 2022, p. 55.
[18] P. Posirisuk, C. Baker, M. Ghajari, Computational prediction of head-ground impact kinematics in e-scooter falls, Accid. Anal. Prev. 167 (2022) 106567, https://doi.org/10.1016/j.aap.2022.106567.
[19] M. Ptak, F. Fernandes, M. Dymek, C. Welter, K. Brodziński, L. Chybowski, Analysis of electric scooter user kinematics after a crash against suv, PLoS ONE 17 (2022) e0262682, https://doi.org/10.1371/journal.pone.0262682.
[20] I. Shichman, O. Shaked, S. Factor, I. Ashkenazi, E. Elbaz, R. Aviv Mordechai, A. Khoury, The association between electric scooter riding position and injury characteristics, J. Saf. Res. (2022), https://doi.org/10.1016/j.jsr.2022.11.009.
[21] Association for the Advancement of Automotive Medicine, Abbreviated Injury Scale: 2015 Revision, 6th ed., Chicago, IL, 2018.
[22] C. Klug, J. Ellway, Pedestrian human model certification technical bulletin 024 v4.0, Tech. Rep., European New Car Assessment Programme (Euro NCAP), 2023.
[23] J. Östh, B. Pipkorn, J. Forsberg, J. Iraeus, Numerical reproducibility of human body model crash simulations, in: Proceedings 21: International Research Council on Biomechanics of Injury Conference, International Research Council on Biomechanics of Injury (IRCOBI), 2021, p. 431.
[24] DYNAmore LS-Dyna Support, Contact modeling in LS-DYNA, 2024.
[25] Toyota Motor, Corporation, Total Human Model for Safety (THUMS) AM50 Pedestrian Model Version 4.02 Documentation, 2021.
[26] C. Got, A. Patel, A. Fayon, C. Tarrière, G. Walfisch, Results of experimental head impacts on cadavers: the various data obtained and their relations to some measured physical parameters, SAE Technical Paper 780887, https://doi.org/10.4271/780887, 1978.
[27] National Highway, Traffic Safety Administration (NHTSA), Occupant Crash Protection, 1972, 49 CFR 571.208, Federal Motor Vehicle Safety Standards.
[28] W. Hayes, M. Erickson, E. Power, Forensic injury biomechanics, Annu. Rev. Biomed. Eng. 9 (2007) 55–86, https://doi.org/10.1146/annurev.bioeng.9.060906.151946.
[29] E.G. Takhounts, M.J. Craig, K. Moorhouse, J. McFadden, V. Hasija, Development of brain injury criteria (bric), Tech. Rep., SAE Technical Paper, 2013.
[30] L. Gabler, J. Crandall, M. Panzer, Development of a second-order system for rapid estimation of maximum brain strain, Ann. Biomed. Eng. 47 (2018), https://doi.org/10.1007/s10439-018-02179-9.
[31] J. Ellway, V. Sandner, A. Eggers, M. Masuda, Brain injury calculation technical bulletin 035 v1.0, Tech. Rep, European New Car Assessment Programme (Euro NCAP), 2022.
[32] G.S. Poplin, T.L. McMurry, J.L. Forman, J. Ash, D.P. Parent, M.J. Craig, E. Song, R. Kent, G. Shaw, J. Crandall, Development of thoracic injury risk functions for the thor atd, Accid. Anal. Prev. 106 (2017) 122–130, https://doi.org/10.1016/j.aap.2017.05.007.
[33] A. Piqueras, J. Iraeus, B. Pipkorn, F.J. López-Valdés, Assessment of the sensitivity of thoracic injury criteria to subject-specific characteristics using human body models, Front. Bioeng. Biotechnol. 11 (2023), https://doi.org/10.3389/fbioe.2023.1106554.
[34] A.M. Nahum, The biomechanics of facial bone fracture, Laryngoscope 85 (1) (1975) 140–156, https://doi.org/10.1288/00005537-197501000-00011.
[35] D.C. Viano, C. Bir, T. Walilko, D. Sherman, Ballistic impact to the forehead, zygoma, and mandible: comparison of human and frangible dummy face biomechanics, J. Trauma Inj. Infect. Crit. Care 56 (6) (2004) 1305–1311, https://doi.org/10.1097/01.ta.0000064209.21216.4e.
[36] J.H. McElhaney, R.H. Hopper, R.W. Nightingale, B.S. Myers, Mechanisms of basilar skull fracture, J. Neurotrauma 12 (4) (1995) 669–678, https://doi.org/10.1089/neu.1995.12.669.
[37] D. Wu, M. Dufournet, J.-L. Martin, Does a full-face helmet effectively protect against facial injuries?, Injury Epidemiology 6 (1) (2019), https://doi.org/10.1186/s40621-019-0197-8.
[38] T.J. Sorenson, V. Borad, W. Schubert, Facial injuries due to cycling are prevalent: improved helmet design offering facial protection is recommended, J. Oral Maxillofac. Surg. 79 (8) (2021) 1731.e1–1731.e8, https://doi.org/10.1016/j.joms.2021.03.013.
[39] R. Stier, P. Jehn, H. Johannsen, C. Müller, N.-C. Gellrich, S. Spalthoff, Reality or wishful thinking: do bicycle helmets prevent facial injuries?, Int. J. Oral Maxillofac. Surg. 48 (9) (2019) 1235–1240, https://doi.org/10.1016/j.ijom.2019.02.018.
[40] National Transportation Safety Board (NTSB) Micromobility, Data Challenges Associated with Assessing the Prevalence and Risk of Electric Scooter and Electric Bicycle Fatalities and Injuries, 2022.